

Dynamic effects in iron phthalocyanine-like compounds

Arūnas Amulevičius*, Kęstutis Mažeika, Vidmantas Remeikis,
Algimantas Undzėnas

*Institute of Physics,
LT-02300 Vilnius, Lithuania*

Received 4 September 2006; accepted 17 January 2007

Abstract: ^{57}Fe isotope-enriched iron phthalocyanine has been synthesized and studied by the Mössbauer spectroscopic method. The samples were investigated in the temperature range 100 – 350 K. Some peculiarities in atomic and molecular electronic structure fluctuations were observed. The intermediate Fe oxidation states are observed and it has been found that the rate of charge redistribution is temperature-dependent. The correlation between the temperature behavior of the isomeric shift and quadrupole splitting has been demonstrated. At elevated temperatures above 300 K, the Fe^{2+} oxidation number is quasistable. The alteration of Fe oxidation number is associated with fluctuations of electron charges, and the electron-accepting and electron-donating properties of surrounding ligands. The energy barriers separating Fe oxidation states have been determined. The possibility of modeling Mössbauer spectra of electron-transfer systems has been shown.

© Versita Warsaw and Springer-Verlag Berlin Heidelberg. All rights reserved.

Keywords: Iron phthalocyanine, Mössbauer spectroscopy, Fe oxidation number, charge distribution, isomeric shift, quadrupole splitting

PACS (2006): 33.45+x, 34.50 Gb, 32.10 Fn

1 Introduction

Conjugated mobile π -electrons in coordination compounds do not belong to a particular atom or bond but are delocalized within the whole system. For these electrons to be promoted to higher orbitals, a small amount of energy is required. The energy of electrons, and electron-electron and electron-lattice interaction energy are major energy types in

* E-mail: antanas@ar.fi.lt

molecular systems. Valence electron densities in coordination compounds under influence of external and internal factors, even at the same chemical (atomic) short-range order, may be distributed in different ways. Metal phthalocyanine complexes with transition elements are thermally very stable. These phthalocyanines are characterized by enhanced electric conductivity and can be used in optoelectronic devices [1–4]. The electron density distribution in molecular bonds predetermines electric, magnetic and optical properties of organic materials [5–8]. Out of a great deal of publications dealing with the Mössbauer effect in coordination compounds, only a small proportion of publications are devoted to iron phthalocyanine. The expected iron oxidation number in such compounds is equal to two, although the postulation of the particular value of this parameter based on an electronic structure of iron atoms is quite problematic. If there are electron-accepting ligands attached to the molecule macrocycle, Fe^{2+} ions along with Fe^{3+} ions are observed in Mössbauer spectra through their respective quadrupole doublets. Mössbauer spectroscopy easily identifies the iron oxidation number since Mössbauer isomeric shift (δ) and quadrupole splitting (ΔQ) values for Fe^{2+} and Fe^{3+} ions differ markedly [9]. It is experimentally possible in iron phthalocyanines to study the electronic density redistribution between iron ions and surrounding nitrogen or other atoms and ligand rings. The main aim of this work was to establish the fluctuating charge states of iron ions, their lifetimes as well as the energy barriers separating ions.

2 Materials and methods

The molecular structure of iron phthalocyanine is presented in Fig. 1. ^{57}Fe phthalocyanine has been synthesized by a procedure described in [10]. At first iron bromide salt was prepared and mixed with urea, phthalic anhydride, sodium sulphate and ammonium molybdate. The mixture obtained was then heated for a couple of hours in the nitrogen atmosphere at 210 – 220 °C. The obtained product was precipitated from the diluted sodium hydroxide solution, washed with ethanol and finally purified several times by sublimation. X-ray diffractograms showed characteristic peaks of β -form crystals. Seeking to lower the statistical dispersion of spectra as well as to improve the precision of Mössbauer spectra parameters, iron enriched with ^{57}Fe up to 20% has been used. Mössbauer spectra were obtained with a conventional spectrometer in transmission geometry. All isomer shifts are given with respect to that of α -Fe at room temperature. Spectra of samples were recorded in a vacuum cryostat at 100 – 350 K. The typical Mössbauer spectra are presented in Fig. 3. The spectra of our samples are different from those recorded by other investigators. According to [11], iron phthalocyanine is in the form Fe^{2+} at room and liquid nitrogen temperatures, whereas in our case this form accounted for about 70% and we had a spectrum with clearly mixed valence states of Fe^{2+} and Fe^{3+} , in addition at temperatures 100 – 300 K we observe the paramagnetic hyperfine structure on the Fe^{3+} ion nuclei. The observed 55T field corresponds to Fe^{3+} ions and its strength cannot be associated with nanoparticles of free iron or its oxides. This type of the spectral structure at measurement temperatures can be caused only by Fe^{3+} ions, since due to

the frozen orbital moment the spin-lattice interaction is weak and the magnetic moment relaxation is slow. To slow down the spin-spin relaxation branch, the Fe ions should be widely separated and their concentration in the sample should not exceed 0.08 – 0.4 mol. %. These ions can be distributed between molecular layers. Apart from iron, other types of impurities (for instance, Cl) can create acceptor-donor centers responsible for the observed electron transfer in the molecule. Synthesizing such complex systems as iron phthalocyanine unavoidably leads to the formation of various defects. Even thorough purification methods can leave excessive atoms in a molecular structure. We measured only Fe atoms, i.e., their isotope ^{57}Fe , and the partial replacement of iron atoms enabled us to increase the spectral sensitivity of the nonstructural iron by about 60 times.

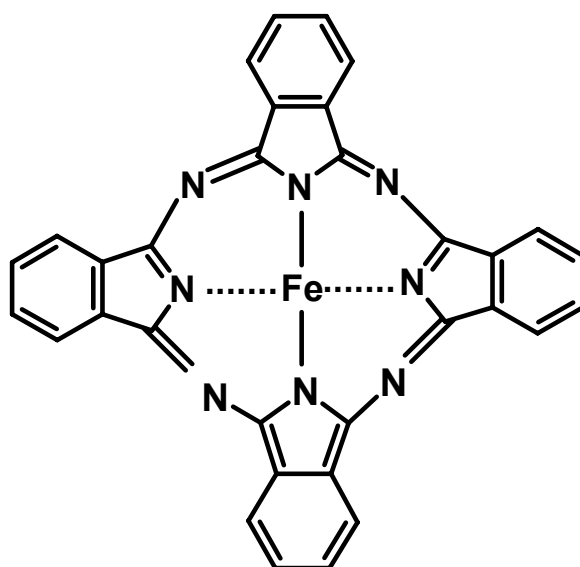


Fig. 1 Molecular structure of iron phthalocyanine.

In our case, the excessive Fe ions are chaotically distributed and their number is small, so they are not recorded in X-ray diffractograms. In the oxidized sample an additional line is observed corresponding to the Fe environment and accounting for the oxygen bond between molecular layers. According to X-ray diffraction insignificant changes in the crystal structure are observed although 0.3 moles of oxygen are incorporated into each mole of iron phthalocyanine [8].

The non-uniform distribution of ^{57}Fe atoms in the sample can be the reason for the spectral anomaly in our case. Since in the natural iron there is only 2.19% of ^{57}Fe , a small concentration of non-uniformities or a small amount of somehow formed $^{57}\text{Fe}^{3+}$ ions ($\leq 1\%$) can be distinctly seen in spectra. Regardless of possible structural anomalies, the Mössbauer isomeric shifts and quadrupole splitting of Fe^{2+} and Fe^{3+} ions corresponded to their typical values usually observed in iron phthalocyanine, and the population of iron valence states was temperature-dependent.

The question arises: are there several Fe environments or does the electron exchange between ions Fe^{2+} and Fe^{3+} take place. In the latter case, the parameters of an interme-

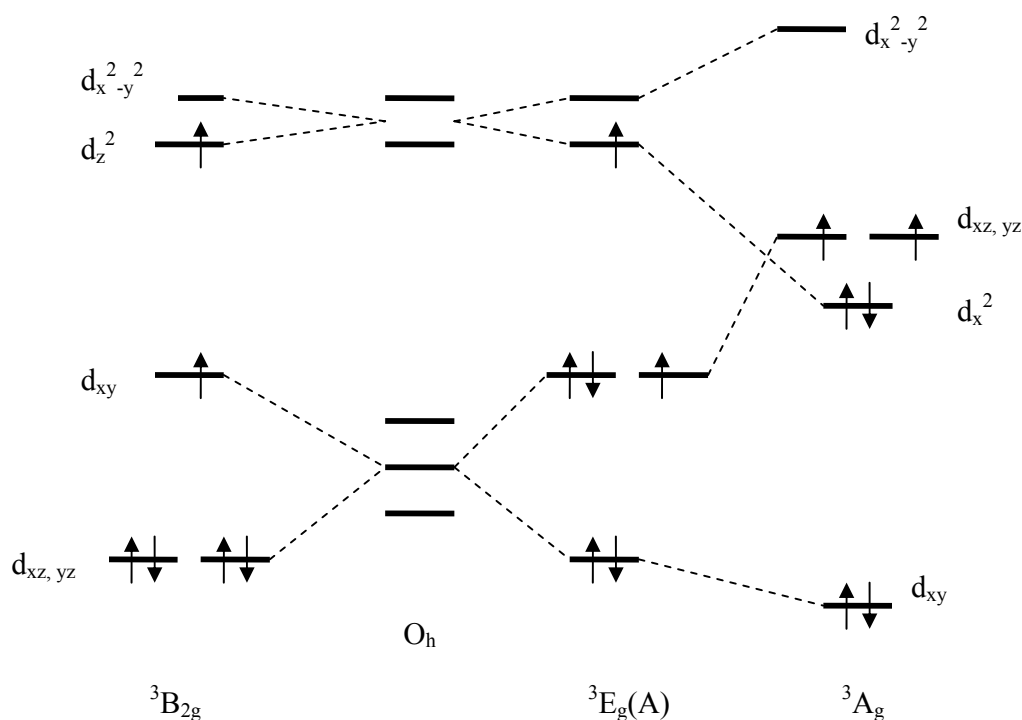


Fig. 2 Three possible electronic spin configurations for the iron phthalocyanine molecule.

intermediate phase should be in-between those of pure phases, and the population of pure phases should comply with obtained parameters of an intermediate phase. They are linked with the transition frequency that predetermines population ratios and the line-width of observed ionic states. In the case of different environments of Fe, we would not observe the intermediate states and the temperature-dependent population of states.

We suppose that regardless of applied purification procedures some electron-accepting and electron-donating admixtures remained in our samples. These admixtures can cause the electron transfer in both directions within the Fe ion-ligand chain. This presumption denies the ion non-uniform distribution version and satisfies the experimentally obtained temperature dependencies of valence state populations. The obtained electronic delocalization is rather large and the lifetime of separate ionic states as compared to the characteristic Mössbauer time is such that separate oxidation states (3+ and 2+) and the averaged 2.5+ virtual state are being observed.

The isomeric shift reflects the s electron density changes at the Fe nucleus. The δ value tells us nothing directly about a $4s$ electron number in the atom since a portion of $4s$ electron charge is screened by $3d$ electrons. As direct quantum-mechanical calculations are rather complex, we shall make use of the following quasiempirical expression to describe the relationship between Δn_{3d} , Δn_{4s} and $\Delta\delta$ [12]:

$$\Delta\delta = -2.05\Delta n_{4s} + 1.25\Delta n_{3d}, \quad (1)$$

where $\Delta\delta$ is the change in the Mössbauer isomer shift caused by changes in the number

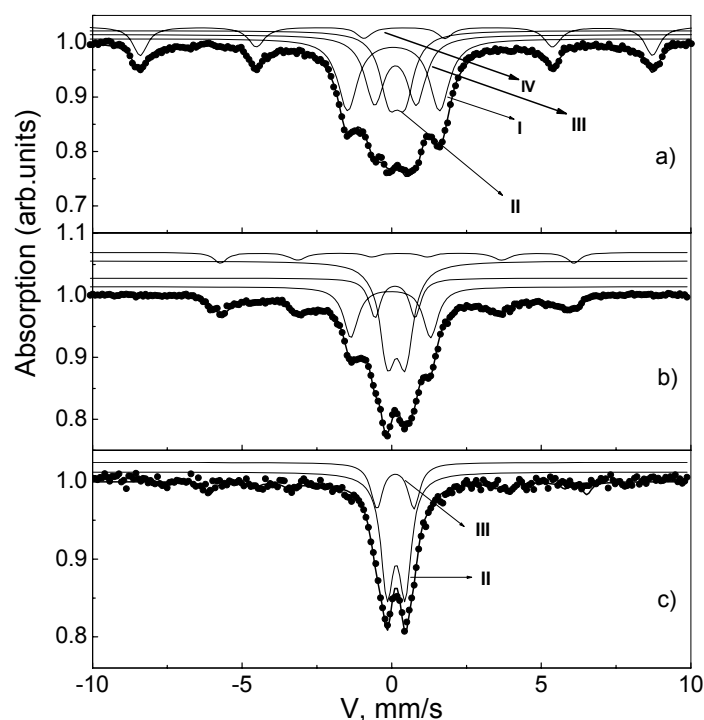


Fig. 3 Mössbauer spectra of the sample obtained at 100 K (a), 300 K (b), 340 K (c): I-IV – subspectra for Fe of various oxidation numbers (I – Fe^{2+} , II – Fe^{3+} , III – $\text{Fe}^{2.5+}$, IV – magnetic splitting subspectra). Points – experimental data. Solid lines represent the best fit.

of 4s or 3d electrons in the Fe atom. The coupling constant for isomeric shift is -2.05 mm/s for one 4s electron and $+1.25$ mm/s for one 3d electron. The δ value is smaller, the larger the selectron density at its nucleus. Expression (1) reflects the change of δ that is caused by the 4s electron density alteration on the nucleus. We assume that δ values are dependent on the 4s electron density on a nucleus as well as on the 4s electron density screening by the 3d electron charge. We suppose that this expression is also valid for molecular crystals.

In fact, the measured resonance line position (CS) is not a pure isomer shift (δ) but is a linear combination of δ and the temperature-dependent second order Doppler shift (SOD):

$$\text{CS} = \delta + \text{SOD}. \quad (2)$$

The SOD arises from the relative motion due to atomic vibrations via a second order relativistic effect: $\text{SOD} = -\langle v^2 \rangle / 2c$, where $\langle v^2 \rangle$ is the mean square velocity of the probe nucleus in the sample. SOD can be calculated using a simple model of atomic vibrations, such as the Debye model [13].

SOD manifests itself in the sample as well as in the Mössbauer source. When Debye temperatures are equal, both SODs are compensated at equal temperatures of the sample and source. The two-band model associated with the Mössbauer effect probability in

molecular crystals has been applied [13] and two Debye temperatures have been obtained. One temperature ($\Theta_1 = 400 \pm 20$ K) describes the motion of Fe within a molecule, the second ($\Theta_2 \approx 50 \pm 10$ K) describes the mutual motion of molecules. The SOD values are practically predetermined by interatomic high-frequency vibrations, i.e. the vibrations of Fe ions within the molecule are described by Debye temperature Θ_1 . In our case the Debye temperatures of the sample and source are about 400 K, and we can assume the SOD value at 300 K to be close to zero, i.e. it is compensated. Using expressions from [13], we evaluated the SOD-caused corrections for δ measured at 100, 220 and 350 K, which are accounted for in Fig. 4.

The mathematical processing of Mössbauer spectra showed that they can be approximated by three quadrupole doublets with broadened lines. Two doublets are assigned to paramagnetic iron ions Fe^{2+} and Fe^{3+} , and the third one is associated with a fast electron exchange between iron ions. The parameters of the third Mössbauer doublet should be intermediate between those of Fe^{2+} and Fe^{3+} and are dependent on the population of the ionic states in a sample. The quadrupole splitting of the third virtual doublet ΔQ_3 can be expressed by the following simple relationship:

$$\Delta Q_3 = \Delta Q_1 p_1 + \Delta Q_2 p_2, \quad (3)$$

where ΔQ_1 and ΔQ_2 are the quadrupole splitting values of ions Fe^{2+} and Fe^{3+} , and p_1 and p_2 are respective ion populations. The normalization condition is $p_1 + p_2 = 1$. Introducing experimentally determined parameters into these expressions enables us to evaluate the ion population probabilities. We use a simple expression to estimate the line broadening $\Delta\Gamma$:

$$\Delta\Gamma = \Gamma_{exp} - (\Gamma_{app} + \Gamma_{nat}), \quad (4)$$

where Γ_{exp} is the experimentally determined line-width. The apparatus line-width was $\Gamma_{app} = 0.05$ mm/s. The natural line-width Γ_{nat} is 0.2 mm/s. All calculated results and Γ_{exp} values are listed in Table 1. One can find lifetimes τ of both ionic states from the Heisenberg uncertainty principle which gives $\Gamma = \hbar/\tau$.

The energy barrier ΔE separating both ionic species can be evaluated by the expression

$$\tau = \tau_0 \exp(\Delta E/kT), \quad (5)$$

where τ_0 is the transfer attempt time and is approximately equal to the lattice vibration period ($10^{-12} - 10^{-13}$ s).

The structure of the Fe^{2+} phthalocyanine complex presented in Fig. 1 is a good example of Fe^{2+} being in a quadratic planar coordination. The expected electronic configurations of the Fe ion are presented in Fig. 2 [9]. More detailed consideration of the configurations will be presented later. Mössbauer spectroscopy is helpful in elucidating the ion electronic properties. This is important for understanding the structure of iron heme proteins and their functioning in live organisms.

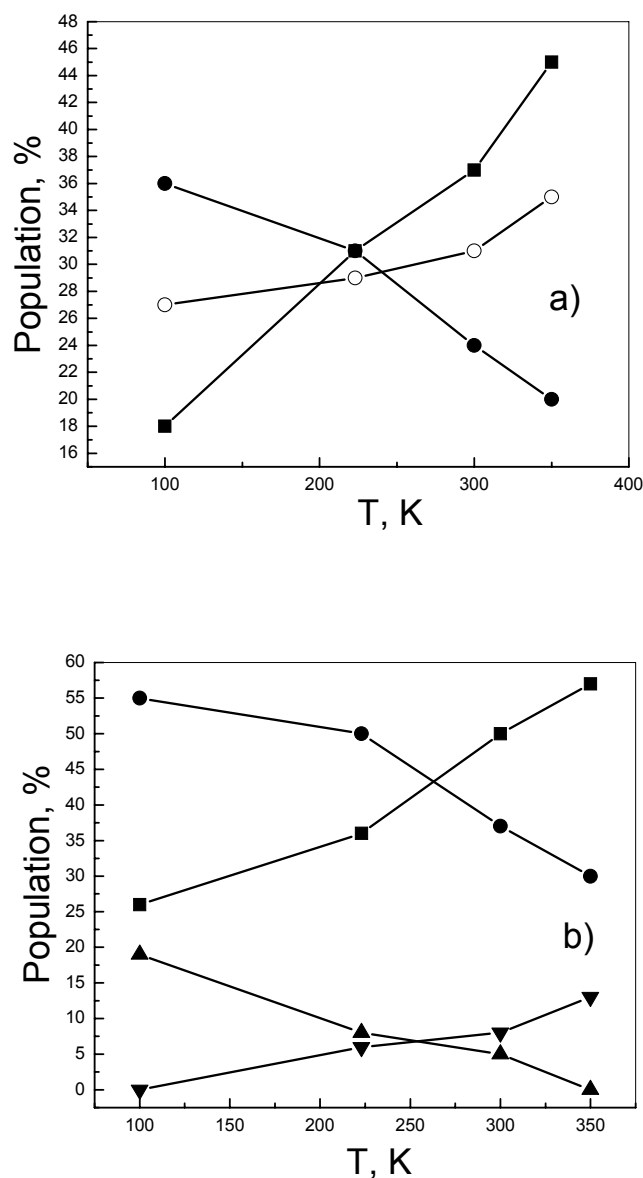


Fig. 4 Experimental populations of Fe²⁺ (●), Fe³⁺ (■) and Fe^{2.5+} (○) (a), and the experimental normalized populations of Fe²⁺, Fe³⁺ ionic states at different temperatures (b). The distribution of excessive atoms in the sample: ▲ – populations of the spectrum magnetic part, ▼ – the amount of excessive Fe³⁺ ions.

The Mössbauer parameters in coordinated compounds are known to be dependent on the ion spin state, valence and environmental coordination [11]. Comparing our parameters with those presented in [11], we have found that the electron spin population of *d* orbitals differs from that required by the simplest theory. Instead of the low-spin state ($S = 0$), the Fe²⁺ ion spin state is intermediate with $S = 1$, and in Fe³⁺ instead of $S = 1/2$, we have the high-spin state $S = 5/2$. This discrepancy shows that *d* orbitals are populated “nontraditionally”, and their splitting in a crystalline field differs from expected splitting in classic phthalocyanine. This crystalline field can be affected by small changes

of the lattice symmetry or by admixtures. We would like to note that in order to describe the spectrum and its temperature dependence, one should introduce the dynamic electron transfer between ions and the virtual $\text{Fe}^{2.5+}$ oxidation state of Fe.

There had been and continues to be at present significant contradictions as to the ground state of an iron ion electronic structure created by side ligands in metal phthalocyanines. The degeneration of octahedral orbitals t_{2g} and e_g is lifted when the environment symmetry degrades from octahedral to square planar. The final arrangement is associated with the relationship between π and σ bonds. There are three possible configurations of three $3d$ orbitals [9]. One of these configurations follows from previous magnetic experiments indicating the intermediate field structure with $S = 1$ spin state and two unpaired electrons. Unfortunately, the various procedures and methods used lead to different answers regarding this problem. Nuclear magnetic resonance and magnetization studies tend to the 3A_g ground state that is widely accepted in molecular orbital calculations. The low-temperature magnetization and paramagnetic anisotropy studies suggest the ${}^3B_{2g}$ ground state. Recording Mössbauer spectra in the external field as well as low-temperature magnetic investigations indicate the presence of the ${}^3E_g(A)$ ground state. By comparing d_{xy} , d_{yz} and d_z^2 populations, only the ${}^3E_g(A)$ ground state satisfies the experimental data (Fig. 2). The experimentally observed non-zero $d_{x^2-y^2}$ orbital population is associated with the iron covalency in phthalocyanine bonds.

The analysis of the Mössbauer spectra has shown that the ions in phthalocyanine are initially in the Fe^{2+} state, although with a portion of ions in the Fe^{3+} state. Usually the electron exchange mechanism implies the electron transfer as a change of a charge and a spin state. This is easily explained when the spin states undergo changes such as $0 \leftrightarrow 1/2$, $1/2 \leftrightarrow 1$, $3/2 \leftrightarrow 2$ and $2 \leftrightarrow 5/2$. In our case, the change involves $1 \leftrightarrow 5/2$ spin states. This process requires the electron charge transfer and spin reorientation. When the spin state 1 loses an electron ($1 \rightarrow e$), it becomes the $1/2$ state, when it acquires an electron ($1 \leftarrow e$), it becomes the $3/2$ state. Accordingly, the process $5/2 \rightarrow e$ leads to the spin state 2 and should rearrange to the spin state $3/2$, i.e., one of electronic levels should become paired and the state $5/2$ becomes the state 1. This is associated with peculiarities of the charge spin distribution in Fe^{2+} and Fe^{3+} ions (Fig. 6).

2.1 Peculiarities of the electron transfer

The spectrum structure of mixed valence compounds depends on the ratio between the observation time and the state lifetime. The characteristic observation time in Mössbauer spectroscopy is the lifetime of the excited nucleus. For ${}^{57}\text{Fe}$ it is 97.8 ns. The Mössbauer spectrum parameters depend on the configuration of ion surrounding electrons and their interaction with a nucleus, whereas the spectroscopic method is sensitive to environment only during the characteristic observation time.

Three cases are possible in our spectra. The first one is when the interatomic charge transfer is slow as opposed to the Mössbauer timescale and the nucleus feels only one valence state. It is possible that the Mössbauer spectrum is the superposition of separate

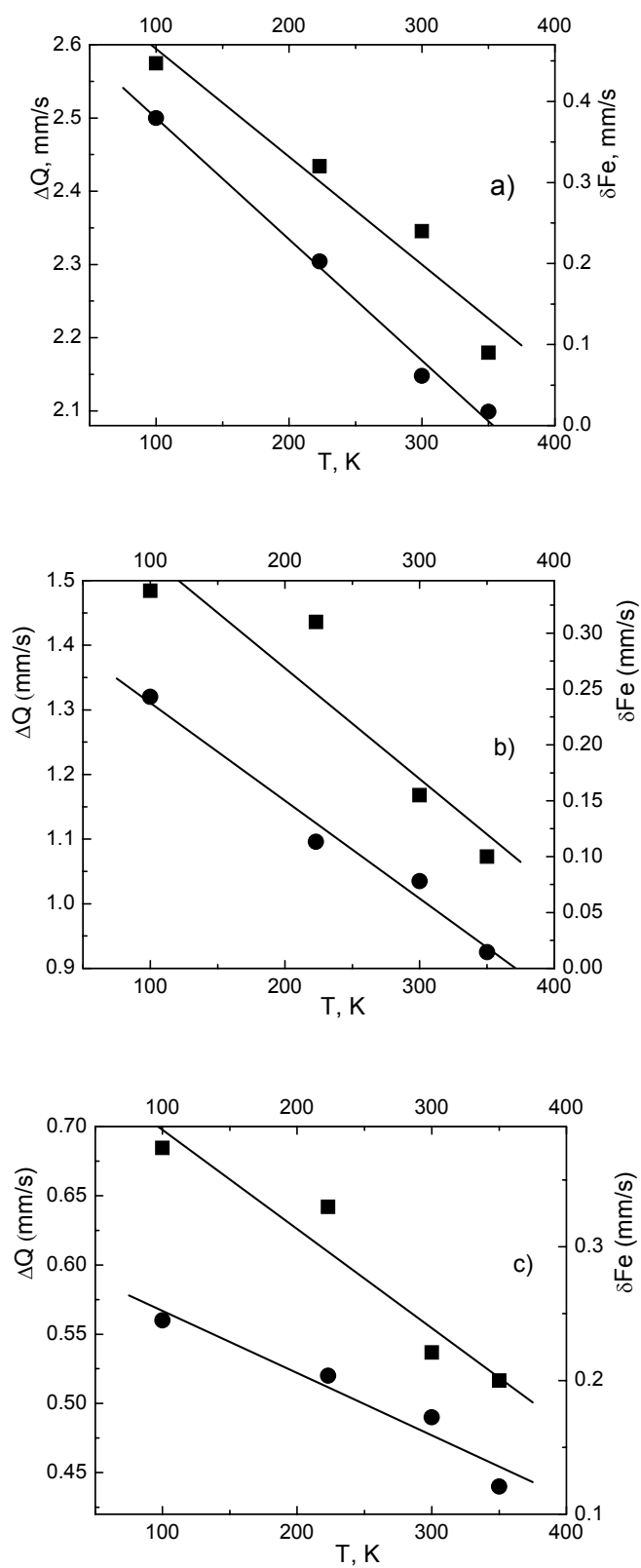


Fig. 5 The temperature dependence of the isomeric shift δ (■) and quadrupole splitting ΔQ (●) for a) Fe^{2+} , b) $\text{Fe}^{2.5+}$, c) Fe^{3+} ions.

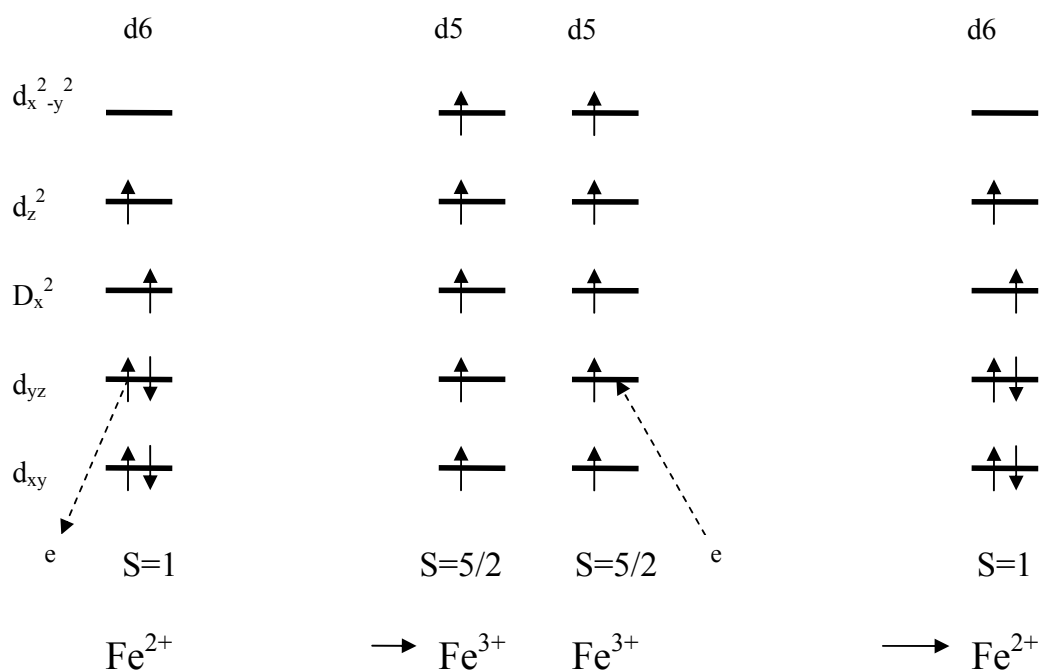


Fig. 6 Possible charge and spin states of (Fe^{3+}) and (Fe^{2+}) iron ions.

Fe^{2+} and Fe^{3+} states (Fig. 7 a). The second one is when the Mössbauer timescale and duration of the interatomic charge transfer are comparable, then discrete and averaged valence states can be observed (Fig. 7 b-e). In the third case, the charge transfer is fast as compared to the Mössbauer timescale, and then only an averaged spectrum of all valence states will be observed (Fig. 7 f).

We shall describe this electron transfer process using a two-state relaxation model [14]. We shall solve the relaxation problem for two formal line pairs AB and CD corresponding to quadrupole splitting lines of Fe^{2+} and Fe^{3+} , although the transfer between doublets AD and BC will be observed as a result of valence state changes. The solution scheme is presented in Fig. 7 a. Lines A,B and C,D approach each other and get broader until they merge into lines E and F of the virtual doublet $\text{Fe}^{2.5+}$ when the valence state change rate increases.

The location of the first two lines A and B can be written as $\omega_A = \delta_1 - \Delta Q_1/2$ and $\omega_B = \delta_2 - \Delta Q_2/2$, and the location of another pair as $\omega_C = \delta_1 + \Delta Q_1/2$ and $\omega_D = \delta_2 + \Delta Q_2/2$. Here $\Delta Q_{1,2}$ is the quadrupole splitting and $\delta_{1,2}$ is the isomeric shift values for Fe^{2+} and Fe^{3+} .

The relative values of W_1 and W_2 define the Boltzmann temperature dependence of populations, and the condition for the free-state population is $W_1 p_{12} = W_2 p_{21}$, where p_{12} , p_{21} are the transfer frequencies of an electronic charge. The peak shape of each line pair, when the transfer is taking place, can be expressed as follows:

$$I(\omega) = 2\text{Re} \left(\frac{i(\omega' + \eta\delta'_i) + 2p}{(\delta_i'^2 - \omega'^2) + 2pi(\omega' - \eta\delta'_i)} \right), \quad (6)$$

where $\omega' = \omega - \omega_i - i\Gamma$, ω_i is the center locations of line pairs AB and CD, and the distances between formal doublet lines are $2\delta_1$ and $2\delta_2$ when there is no transfer, Γ is the line-width. The population relative difference $\eta = (W_1 - W_2)/(W_1 + W_2) = (p_{21} - p_{12})/(p_{21} + p_{12})$ determines the location of lines E and F. The relaxation rate is $2p = p_{12} + p_{21}$. The location of lines A, B, C and D is $\omega = \omega_i \pm \delta'_i$ and is determined using parameters of the formal doublets AB and CD.

3 Results and discussion

Vibrations of molecules or their fragments can cause electronic density perturbations in organic molecular systems. The frequency of these processes is in the range 10^{10} – 10^{13} s⁻¹ and the Mössbauer spectra provide a picture of the time-averaged charge redistribution.

At low temperatures ($T < 300$ K), the Mössbauer spectra (Fig. 3) can be approximated by three quadrupole doublets (I-III) and a magnetic sextet (IV). Population probabilities of ion states at various temperatures are presented in Fig. 4. Fe³⁺ and Fe²⁺ populations are renormalized according to paramagnetic sextet dependence upon temperature. When describing Fe³⁺ ion populations in Fig. 4 b, excessive Fe³⁺ ions are taken into account.

Parameters of quadrupole doublets for Fe^{2.5+} are listed in Table 1.

Table 1 Parameters of Fe intermediate oxidation states: 1,2 – experimental values of the Mössbauer isomeric shift (δ) and quadrupole splitting (ΔQ); 3,4 – populations according to the 1,2 data; 5,6 – values of δ_3 and ΔQ_3 are calculated using experimentally determined populations and data of Fe³⁺ and Fe²⁺; 7 – the average line-width of the subspectra lines.

	T , K	100	200	300	340	Error, \pm
1	δ , Fe ^{2.5+} mm/s	0.228	0.255	0.155	0.180	0.02
2	ΔQ , Fe ^{2.5+} mm/s	1.320	1.090	1.030	0.920	0.02
3	p_1 (Fe ³⁺)	0.530	0.360	0.290	0.190	0.02
4	p_2 (Fe ²⁺)	0.470	0.640	0.710	0.810	0.02
5	Γ^{2+}	0.500	0.621	0.740	0.468	0.02
6	$\Gamma^{2.5+}$	0.485	0.605	0.609	0.500	0.02
7	Γ^{3+}	0.438	0.529	0.532	0.432	0.02

Let us assume that the chemical short-range order is the same for all iron ions and is temperature-independent, but the iron oxidation number may change as a result of fluctuations of valence electron charges. The charge fluctuations occur between Fe ions and nitrogen atoms in indole rings.

Δn_{3d} and Δn_{4s} electron number alterations corresponding to experimental values of $\Delta\delta$ at various temperatures are presented in Table 2. Calculations were carried out using expression (1). In an attempt to separate contributions of Δn_{3d} and Δn_{4s} electron charges to alterations of the charge distribution, we perform an analysis of experimental values of quadrupole splitting. The d electron density distribution is spherically symmetrical

and creates no gradient of an electric field (EFG), as well as no quadrupole splitting in the nucleus. ΔQ of Fe^{3+} is caused by the lattice. The main source of the EFG is uncompensated charges of $3d$ electrons. One uncompensated $3d$ electron charge can create an EFG of about $5 \cdot 10^{21}$ V/m². The quadrupole moment of an excited iron nucleus is 0.28 barn ($0.28 \cdot 10^{-28}$ m²) and this field creates a ΔQ of 12.6 mm/s. As can be seen in Fig. 4, the ΔQ values are significantly lower, thus only a portion of the $3d$ electron charge takes part in creating the EFG. Table 1 shows the portion of the $3d$ electron charge participating in creating the EFG corresponding to observed ΔQ values. Having assessed Δn_{3d} , we can easily find Δn_{4s} as well. The data obtained suggest that thermal changes of hyperfine parameters require quite small changes in the electronic density. The interaction of Fe^{3+} ions with phonons is markedly weaker as compared to Fe^{2+} ions.

Table 2 Iron oxidation numbers at different temperatures and changes in $4s$ and $3d$ electron number corresponding to experimental isomeric shift and quadrupole splitting.

T(K)	100	200	300	340
Fe^{2+}	$3d^{5.15}4s^{0.26}$	$3d^{5.14}4s^{0.21}$	$3d^{5.13}4s^{0.10}$	$3d^{5.13}4s^{0.16}$
$\text{Fe}^{2.5+}$	$3d^{5.06}4s^{0.15}$	$3d^{5.04}4s^{0.15}$	$3d^{5.04}4s^{0.10}$	$3d^{5.04}4s^{0.11}$
Fe^{3+}	$3d^5 4s^{0.13}$	$3d^5 4s^{0.13}$	$3d^5 4s^{0.11}$	$3d^5 4s^{0.14}$

Having reached the nitrogen ring, the charge fluctuations can also be transferred to iron ions. Thus, the density alterations of $3d$ or $4s$ electrons in central Fe ions depend upon surrounding axial ligand dynamics as well as on the accepting and donating properties of atoms. The lifetime of various oxidation states is dependent on the height of the separating energy barrier that can be overcome by tunneling. The tunneling process requires exact matching of electronic levels (10^{-7} eV), and as a result the process is very slow. The lattice vibrations broaden the electronic levels up to 0.05–0.1 eV and the charge transfer proceeds quite rapidly.

The simulated spectra describing the shape at various electron transfer times and state populations using expression (6) are presented in Figs. 7 and 8. Fig. 7 a depicts the superposition of two quadrupole doublets corresponding to parameters of Fe^{2+} and Fe^{3+} in phthalocyanine. The populations of both doublets are the same ($\eta = 0$) and the electron transfer time is $\tau = \infty$ (no transfer). The half-width of the spectral lines is $\Gamma = 0.25$ mm/s. Fig. 7 b shows the spectrum when $\eta = 0$ and $\tau = 10^{-7}$ s. The quadrupole splitting of the first doublet decreased, and that of the second one increased by 0,1 -0,2 mm/s. The lines broadened up to 0.59 mm/s. Fig. 7 c presents the spectrum with $\eta = 0$ and $\tau = 8 \cdot 10^{-8}$ s. The doublet lines approach each other and broaden up to 0.71 mm/s as the transfer time gets shorter. In Fig. 7 d the transfer time was reduced to $5 \cdot 10^{-8}$ s. In this case only a doublet with intermediate parameters and with broadened lines ($\Gamma = 0.75$ mm/s) is observed. Figs. 7 e,f show a model spectrum at $\tau = 2 \cdot 10^{-9}$ and 10^{-9} s, which is a doublet. The line half-widths are $\Gamma_e = 0,54$ mm/s and $\Gamma_f = 0,29$ mm/s. One can see that the lines get narrower and their half-width approach the initially set value Γ

= 0.25 mm/s. Fig. 8 shows model spectra at different populations and relaxation times.

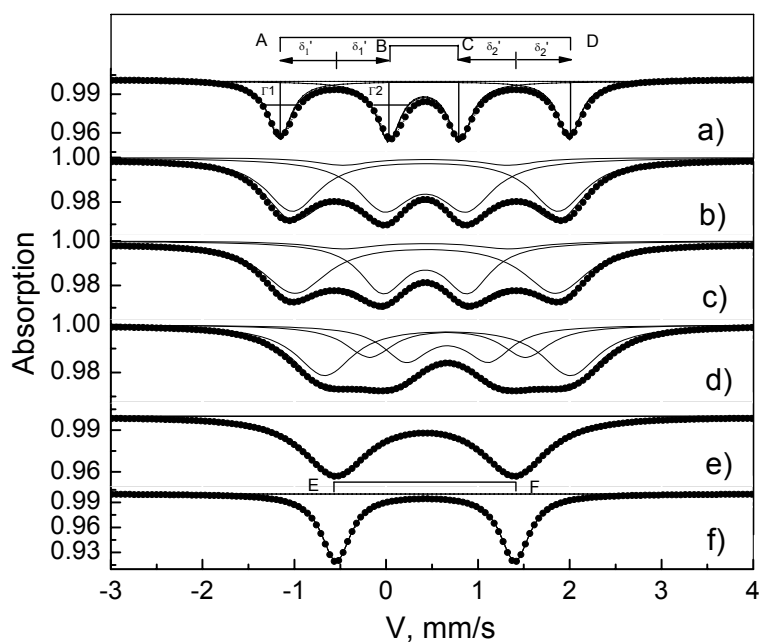


Fig. 7 Mössbauer model spectra: a) the doublet superposition of Fe^{2+} and Fe^{3+} states during the electron transfer; b) $\tau=10^{-7}$ s, $\eta=0$; c) $\tau=8\cdot 10^{-8}$ s, $\eta=0$; d) $\tau=5\cdot 10^{-8}$ s, $\eta=0$; e) $\tau=2\cdot 10^{-9}$ s, $\eta=0$; f) $\tau=10^{-9}$ s, $\eta=0$. The calculation scheme of relaxation spectra is shown in the upper part.

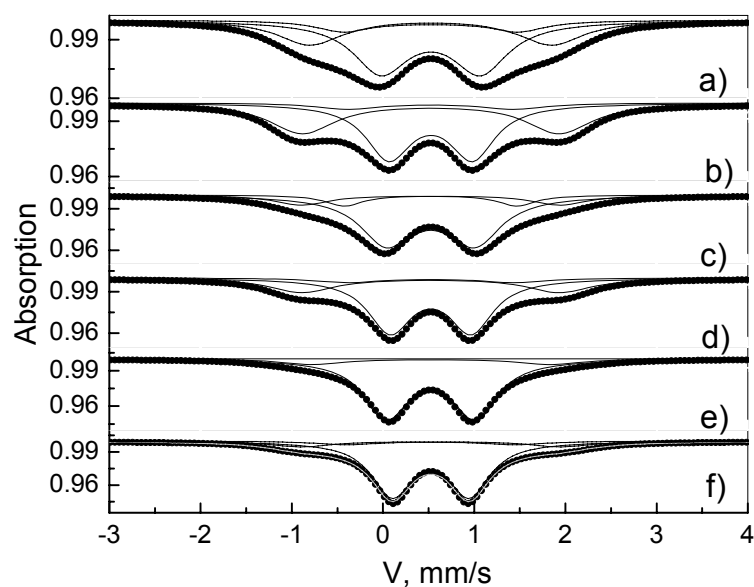


Fig. 8 Mössbauer model spectra at various values of η and τ : a) $\eta=0.2$, $\tau=5\cdot 10^{-8}$ s; b) $\eta=0.2$, $\tau=1.2\cdot 10^{-8}$ s; c) $\eta=0.4$, $\tau=5\cdot 10^{-8}$ s; d) $\eta=0.4$, $\tau=1.25\cdot 10^{-8}$ s; e) $\eta=0.6$, $\tau=5\cdot 10^{-8}$ s; f) $\eta=0.6$, $\tau=1.25\cdot 10^{-8}$ s.

We see that the Fe^{2+} lines are broader, the states are living shorter and the transfer

is faster. In the experimentally obtained spectrum this is associated with the fact that Fe^{2+} ions are interacting with the lattice vibrations much stronger than Fe^{3+} ions since the orbital moment of Fe^{2+} is $L = 2$, and that of Fe^{3+} is $L = 0$ and there is no electron-phonon interaction.

It has been found by comparing model spectra with experimental ones that the electron transfer in our samples occurs with frequency $10^7 - 10^9 \text{ s}^{-1}$. The electron transfer is stimulated by atomic vibrations in the molecule, so we take the pre-exponential term as 10^{-13} s ($\Theta_1 = 400 \text{ K}$), and using expression (5) can find an energy barrier hindering the transfer. Its value is about $0.12 - 0.3 \text{ eV}$ at temperatures $100 - 300 \text{ K}$. This value supports the good semiconducting properties of the compound.

The $\text{Fe}^{2.5+}$ state is not an intermediate $\text{Fe}^{2.5+}$ oxidation state but the state reflecting the electronic charge redistribution between Fe^{2+} and Fe^{3+} ions that occurs in faster than 10^{-7} s^{-1} .

The iron ions are widely separated (about 0.5 nm) and the direct electron exchange is very slow, if any. Two chains are involved in the charge redistribution mechanism: “axial ligands – nitrogen ring” and “nitrogen ring – iron ion”.

The amount of Fe^{2+} drops with the increasing frequency of electronic charge transfer with temperature from 36% (at 100 K) to 20% (350 K). In the electron exchange process, more Fe^{2+} ions will release an electron charge or its part to molecular orbitals with increasing temperature, thus increasing the amount of quasistable Fe^{3+} states. The number of Fe^{3+} ions increases with temperature from 18% (at 100 K) up to 45% (at 350 K) (Fig. 4). The population of the intermediate valence state reaches the 31% value. After cooling down the sample, then warming up and recording the spectrum at room temperature, the state populations are recovered — which demonstrates the dynamic character of the electron transfer phenomena.

3.1 The temperature dependence of Mössbauer parameters of Fe^{2+} , $\text{Fe}^{2.5+}$, Fe^{3+} ions

The appearance of spectral lines of Fe^{3+} ions suggests that electron-donating and electron-accepting properties of ligands can affect the central ion oxidation number. The separating energy barrier determines the lifetime of different oxidation states and it becomes more transparent with increasing temperature. The transition from the Fe^{2+} to Fe^{3+} state takes place during the phonon-assisted activation process via the nitrogen ring.

As seen in Fig. 5 a, b and c, the values of δ and ΔQ of Fe ions increase with lowering temperature. For Fe ions, being of the D_{4h} symmetry, δ and ΔQ increase if σ donation or π back donation of axial ligands decrease. The coupling constant between the number of s electrons and δ is negative, therefore the δ value increases when the s electron density on the nucleus decreases. It is known that δ increases when σ donation decreases or the π back donation increases, i.e. if s electrons are taken off the ion. ΔQ decreases when the δ donation from axial ligands increases or the π donation decreases [15].

4 Conclusions

In summary, ^{57}Fe isotope-enriched β -iron phthalocyanine has been synthesized and studied using the Mössbauer spectroscopic method. It has been found that there is no single stable oxidation number in iron. Iron oxidation numbers observed in Mössbauer spectra are instantaneous. The thermodynamic equilibrium in the charge distribution is attained by virtue of continuous charge redistribution in the Fe-N chain and within the macro-molecule. The rate of charge redistribution is temperature-dependent. The correlation between the temperature behavior of the isomeric shift and quadrupole splitting has been observed. At higher temperatures ($T > 300$ K), the quasistable Fe^{2+} oxidation number is observed. A method of constructing model spectra of the electron transfer has been proposed.

References

- [1] H. Wachtel et al.: “Spin dynamics in oriented lithium phthalocyanine thin films investigated by pulsed electron spin resonance”, *J. Chem. Phys.*, Vol. 102, (1995), pp. 5088–5093.
- [2] Y. Shirota: “Organic materials for electronic and optoelectronic devices”, *J. Mater. Chem.*, Vol. 10, (2000), pp. 1–25.
- [3] G. De la Torre et al.: “Phthalocyanines and related compounds: organic targets for nonlinear optical applications”, *J. Mater. Chem.*, Vol. 8, (1998), pp. 1671–1683.
- [4] M. Tian et al.: “Novel non-aggregated unsymmetrical metallphthalocyanines for second-order nonlinear optics”, *J. Mater. Chem.*, Vol. 7, (1997), pp. 861–863.
- [5] R. Göbl et al.: “Magnetic properties of uranium ferrocyanides and ferricyanides”, *Czech. J. Phys.*, Vol. 50, (2000), pp. 671–676.
- [6] M. Evangelisti et al.: “Magnetic properties of α -iron (II) phthalocyanine”, *Phys. Rev. B*, Vol. 60, (2002), art. 144410.
- [7] V. Gulbinas: “Transient absorption of photoexcited titanylphthalocyanine in various molecular arrangements”, *Chem. Phys.*, Vol. 261, (2000), pp. 469–479.
- [8] E. Kuzmann et al.: “Mössbauer study of oxygenated iron-phthalocyanines, a precursor of magnetic storage material”, *Hyp. Interact.* Vol. 139/140, (2002), pp. 631–639.
- [9] P.E. Dickson and F.J. Berry ed.: *Mössbauer spectroscopy*, Cambridge University Press, Cambridge, 1986.
- [10] V.M. Derkatcheva et al.: “New method of preparing iron phthalocyanine”, *Zh. Neorg. Khim.*, Vol. 26, (1981), pp. 1687–1690 (in Russian).
- [11] I.P. Suzdalev: *Gamma-resonance spectroscopy of proteins and model compounds*, Moscow, Nauka, 1988 (in Russian).
- [12] F. van der Woude and K.W. Maring: “The electronic and magnetic properties of iron-sp element alloys”, In: *Proc. Intern. Confer. on Mössbauer Spectroscopy*, Bucharest, pp. 1132–1161 (1977).
- [13] A. Amulevičius et al.: “Mössbauer effect and dynamics of atoms in iron phthalocya-

- nine“, *Lithuanian J. Phys.*, Vol. 39, (1999), pp. 27–32.
- [14] D.H. Jones and K.K.P. Srivastava: “Many-state relaxation model for the Mössbauer spectra of superparamagnets“, *Phys. Rev. B*, Vol. 34, (1986), pp. 7542–7548.
- [15] H. Inoue et al.: “Mössbauer spectroscopic characterization of iron chlorophyllins“, *Hyp. Interact.*, Vol. 29, (1986), pp. 1403–1406.